Available online at www.CivileJournal.org

Civil Engineering Journal

(E-ISSN: 2476-3055; ISSN: 2676-6957)

Vol. 11, No. 05, May, 2025

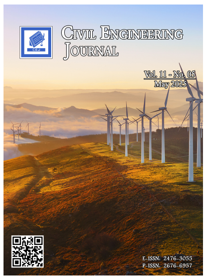

Infrared Thermal Monitoring of Intersection Elements of Urban Road Infrastructure and Road Traffic Via Drone

Iliyan Damyanov [1*], Georgi Mladenov [1], Durhan Saliev [1], Rosen Miletiev [2], Kalin Dimitrov [2], Vladimir Hristov [3]

[1] *Faculty of Transport, Technical University of Sofia, 1756 Sofia, Bulgaria.*

[2] *Faculty of Telecommunication, Technical University of Sofia, 1000 Sofia, Bulgaria.*

[3] *Faculty of Automatics, Technical University of Sofia, 1000 Sofia, Bulgaria.*

Received 15 February 2025; Revised 22 April 2025; Accepted 27 April 2025; Published 01 May 2025

Abstract

This paper presents a thermographic analysis of a street junction within an urban road network, focusing on identifying thermal load sources generated by vehicle traffic—an increasingly significant environmental concern for urban populations. The study explores the application of thermographic methods at urban intersections and the creation of thermal maps. These approaches support the advancement of intelligent transport systems, aligning with smart city initiatives aimed at optimizing traffic flow management. Additionally, the findings provide potential for assessing the conditions of both road transport infrastructure and vehicles. By adopting this comprehensive perspective for monitoring urban environments and transportation systems, cities can enhance overall quality of life and public well-being. The results emphasize the value of conducting broad-scope studies, suggesting that combining ground-based and aerial thermal imaging leads to more informed decision-making.

Keywords: Monitoring of the Urban Environment; Temperature Load; Thermographic Survey and Research; Thermal Imaging; Transport System Management.

1. Introduction

An increasing amount of street traffic and the related issues necessitate innovative approaches and tools to examine key factors and patterns, ensure proper and safe road traffic management, and reduce its environmental and social impacts. Research and analysis of thermal methods applied to crossroads as components of urban networks, vehicles, transport infrastructure, and intelligent management are still in the early stages of development. The interest in such research is driven by the need to ascertain, diagnose, and control the condition of road infrastructure based on the thermal load resulting from road traffic:

- State of the Art in Describing Parameters of Road Transport Infrastructure Based on Its Thermal Load from Road Traffic;
- An increase in temperature load in urban environments due to vehicle traffic, which poses a serious environmental and thermal threat to the population in cities, especially during the summer season, considering global warming over the last few decades;

* Corresponding author: idamyanov@tu-sofia.bg

http://dx.doi.org/10.28991/CEJ-2025-011-05-02

- Assessing the condition of vehicles based on the heat energy released while waiting at and passing through intersections, as well as enabling the potential detection of traffic accidents that have occurred. This leads to enhanced traffic safety levels and better organization and control of road traffic.

The thermography may only be used to detect (localize) irregularities caused by both the load of road vehicles on the road surface and the temperature load during the hottest days of summer when employing unmanned aerial vehicles and aerial photography. This approach is highly suitable for this type of research in the city's busy street network.

The study confirms the potential for examining the thermal load of both road infrastructure and the heat emitted by vehicles using an unmanned aerial vehicle equipped with a thermal camera. Therefore, the study will evaluate the entire system of infrastructure and vehicles to recommend measures for reducing thermal load on both road surfaces (including materials) and the urban environment, as well as for pedestrians in urban areas. This analysis will clarify the elements of the city's street network, such as traffic lights, road types, lane numbers, lawns, buildings, and more, that require specific measures. No similar studies or analyses have been conducted in Bulgaria, or at least this has not come to the authors' attention at the time of writing this article. This fact, in itself, inspired our study.

2. Materials and Literature Review

Heat stress stands as one of the typical harmful and dangerous emissions to which we are continually exposed. Regular and prolonged exposure to increased heat loads brings in place diverse forms of adverse health outcomes. Heat stress stands as one of the typical harmful and dangerous emissions to which we are continually exposed. Regular and prolonged exposure to increased heat loads brings in place diverse forms of adverse health outcomes. The number of people exposed to extreme heat is reported to be on an exponential rise as indicated by climate change phenomena across all regions of the world, according to [1].

Between the periods 2000–2004 and 2017–2021, heat-related mortality among individuals aged 65 and over increased by approximately 85%. Research indicates that from 2000 to 2019, there were an estimated 489,000 heat-related deaths annually, with Asia accounting for 45% and Europe for 36% of these fatalities [2]. Notably, the summer of 2022 alone witnessed 61,672 excess heat-related deaths in Europe, underscoring the growing public health impact of extreme temperatures. High-intensity heat waves may lead to significant acute mortality, as evidenced by the 70,000 deaths recorded from June to August 2003 in Europe. In the Russian Federation, over 56,000 deaths occurred during a 44-day heat wave in 2010 [3]. Individual vulnerability to heat due to physiological or clinical factors in adults is well documented. The vulnerability of adults to heat has been thoroughly characterized by both physiological and clinical factors [4]. Limited research exists on the effects of chronic (long-term) exposure to high temperatures and humidity. Another area that requires research and analysis is the heat load from traffic on the urban street network, particularly concerning the so-called heat islands in developed cities.

Road infrastructure is essential for the socioeconomic development of any country, providing passenger and goods services while facilitating the construction, maintenance, and repair of this infrastructure. The rapid growth of global travel connections, combined with the increasing frequency of vehicle use in cities, leads to a significant rise in heat emissions, which is linked to the condition of the vehicles and their equipment.

A review of existing research in this complex field reveals that many studies tend to focus in depth on only one or a limited number of the key directions necessary for addressing the broader challenges. Overall, the research in this domain can be categorized into two main areas: state-oriented efforts, which encompass both the construction and operational aspects of urban infrastructure, and scientific research, which aims to develop new methods, technologies, and analytical frameworks to support effective monitoring and management.

Studies are primarily funded and supported by state institutions. These studies often focus on the development and execution of road infrastructure, especially the quality of implementation carried out by relevant state bodies. Because information from these studies is either partially available or unofficially published, the collected content tends to be fragmentary and vague, with limited data to substantiate it, primarily intended for internal use [5, 6]. Another segment of such studies is conducted by the road owner or infrastructure concessionaire (lessee). Since these studies take place within the infrastructure's operation, the information gathered is primarily for the road owner and is only partially shared with the public, typically through media outlets [7]. The research in this field mainly concerns the state of road infrastructure, and for the region of the Republic of Bulgaria, strategies and visions for development are often discussed without actionable results. Notably, some studies concentrate on the costs of infrastructure and their correlation with unemployment [8] and the impact of climatic conditions on road infrastructure [9-12]. A substantial amount of research has addressed the management of risks and vulnerabilities in the road transport network. Other researchers have explored issues and perceptions— as well as comfort— related to the state of road transport infrastructure. Additionally, research exists regarding how the state of road transport infrastructure affects the movement of goods and freight in terms of economic indicators, observed at both national and regional levels, particularly in urban environments. A specific area with designated connectivity directly relates to the road network's condition. This is evident in the easier access to routes that facilitate shorter travel times to reach destinations [13-16]. Furthermore, there is a substantial number of studies examining the impact of transport and related activities on air pollution, which affects the health of urban residents [17]. Many studies evaluate the health risks associated with transportation- related pollution and the policies and strategies designed to mitigate these risks in urban settings [18, 19]. However, a significant portion of these studies has primarily focused on road safety and measures to decrease road traffic accidents [20]. These measurements are often implemented by researchers, government departments and ministries, and medical and paramedical assistance following road accidents [21, 22], as well as collaboratively between institutions and researchers from various fields [23, 24].

Another group of researchers focused their study on materials used in the production and mixing of asphalt mixtures and ways to improve their quality. They examined the factors that influence the efficiency of asphalt concrete pavements against climate-induced deformation. Since asphalt road surfaces are directly exposed to atmospheric conditions, the characteristics of asphalt concrete pavements depend on the behavior of bitumen. Bitumen is a complex material that demonstrates different behaviors depending on its temperature. At high temperatures, it acts like a liquid; at intermediate temperatures, it can be considered a viscoelastic material; and at low temperatures, it may be regarded as a viscoelastic solid [25-28].

The challenges of climate change, alongside the general trend of rising temperatures worldwide, will inevitably impact the service life of pavements, as noted in most reports [29]. This study on climate change for US conditions indicated that fatigue is expected to increase by 2–9% and rutting by 9–40% by the end of 20 years [30]. Other authors have examined deformations and distortions of tracks, which are the most frequently observed initial distresses in asphalt pavements [31]. Additionally, infrared thermography is used to assess damages in concrete and asphalt pavements, such as debonding, delamination, and voids, etc. [32-34]. A recent study has demonstrated that infrared thermography can detect debonding defects when there is a temperature difference of over 0.5 °C at the bonded area and that damage does not extend deeper than 50 mm [35]. Several researchers have concentrated on discovering new methods for mixing, curing, and utilizing various additives in asphalt mixtures to enhance quality, durability, and temperature resistance of asphalt mixtures used as road surfaces.

The study work using IR thermography focuses both on the surface of the pavement itself during the concerned operation and on transportation from the asphalt bases with vehicles [37-39], whether suitable or not. It also examines the laying of the pavements themselves to achieve uniform cooling, which depends on the quality and durability of the laid pavement [40, 41].

To enhance the quality and longevity of road surfaces, some authors propose using temperature measurement through infrared thermography and machine intelligence for effective transportation and laying methods [42, 43]. The majority of studies focus on bridges, concrete structures, and bridge facilities, utilizing both ground surveys and aerial assessments [44-47]. Other researchers advocate for the application of ground-based photography and aerial drones equipped with thermal cameras for similar investigations, indicating comparable reliability in thermal research [48-51].

Research on global warming, specifically regarding the increased temperature load in urban environments, has utilized infrared thermography over the past few decades. This research examined pavements, buildings, and materials used in urban infrastructure through the lens of creating a livable environment and heat absorption. In Yamazaki et al. [52], the authors conducted their urban heat island (UHI) study in Tokyo, Japan, using thermal images. Their results indicated that the surface temperatures of asphalt roads were significantly higher than those of any other type of pavement. The study also found that areas with roadside trees and plants, devoid of buildings, were cooler than those with pavement or building walls. The greening of urban rooftops as part of smart city initiatives has been researched for its mitigation effects using aerial thermal cameras (via helicopter). The influence of wetlands and grassy areas on the effects of rising temperatures in urban settings has also been thoroughly investigated and confirmed [53-56]. Additionally, the effects of urban heat islands—specifically CO_2 emissions from these islands and the climatic impacts of rising air temperatures in cities on residential areas- are well-studied issues as well [57].

From the perspective of using infrared thermography to assess the technical condition of road vehicles based on heat energy emissions during their time at crossroads and while passing through, it is not easily traceable if this trend is considered regarding the research experiences in this field. The general research diverges from merely precise temperature measurements at the workplace, encompassing both driver behavior and working conditions, as well as driver temperature and perception. A method for measuring temperature on the windshield area of an automobile has been developed and further modified according to European de-fogging standards (CEE 78/317) to enhance the driver's thermal comfort and driving control. Likewise, many studies utilize IRT (Infrared Thermography) as presented in this study, but specifically for diagnosing and determining the technical condition of individual components, aggregates, or groups of elements, primarily concerning the condition of the vehicle’s interior or under bench conditions [58, 59]. Other studies on IRT focus on vehicle detection in low visibility conditions, like night time, and other compromised video surveillance settings to monitor traffic flows on streets, as well as to detect and recognize various electric and conventional vehicle categories using thermal video cameras [60, 61]. Furthermore, several approaches have been combined for vehicle research and detection within traffic monitoring. Some studies also examine the use of IRT for driving autonomous vehicles and identifying hazardous situations related to traffic accidents and object movements, particularly under low visibility conditions such as fog and snow, as well as at night [62-64]. Authors in previous studies propose road patrolling via Unmanned Aerial Vehicles with IRT as a strategy to reduce road fatalities by detecting traffic accidents [65, 66].

From the analysis, it is clear that many authors conduct in-depth research and analysis on only one or a few of the topic areas that the current team intends to explore. This is a multi-faceted and complex task that requires fostering teamwork while drawing on knowledge and skills from various fields. The researchers who contributed to the development of the study have accumulated years of experience relevant to the study's objectives, which are:

To study the effects of road traffic at a crowded road intersection in Sofia, Bulgaria, using aerial photographs taken with a drone equipped with both thermal and standard cameras. From these aerial images, photogrammetry software will be utilized to create a heat map of the intersection and the buildings in the surrounding area, to:

- Monitor how automobile traffic impacts the condition of buildings and the quality of road transport structures.
- Determine if it is possible to assess the technical state of passing vehicles from thermal images.
- Measure the temperature impact of vehicular traffic on the well-being of residents and visitors to the town.
- Consider the overall thermal condition of nearby structures that fall within the intersection's area.

With increased emphasis on traffic and infrastructural issues and the impact of vehicular traffic in large cities, there is growing interest in thermal remote sensing applications within urban environments. In the research described, infrared thermography was employed as a relatively new yet highly effective and versatile tool for non-destructive control and diagnostics. It enables the identification of specific problems before they jeopardize road traffic safety or result in material damage and financial losses. The results of infrared thermography can provide a qualitative assessment of the technical condition of road infrastructure and vehicles; this information lays the groundwork for implementing effective programs for preliminary monitoring and maintenance of both the infrastructure and the vehicles, as well as monitoring and controlling the total temperature load of the examined road transport node (intersection or road section).

3. Methods and Results

The aerial photography to gather information about thermal load in the street network is likely to succeed. The main advantage of using UAVs (Unmanned Aerial Vehicles) is that the photography occurs from the air, eliminating the need to stop traffic, as would be required with ground photography of the pavement. The rapid advancement of the technology and equipment for unmanned aerial vehicles enhances the ability to determine the thermal characteristics of drones, as these devices are already commonly equipped with thermal cameras.

For this study, the DJI Mavic 2 Enterprise Advanced [67] was chosen as the aerial thermographic platform. This professional unmanned aerial vehicle (UAV) combines a high-resolution visual (RGB) camera and a radiometric thermal imaging sensor, facilitating detailed thermal data collection from various altitudes. The technical specifications of the onboard thermal camera are outlined in Table 1, alongside a description of the monitored location—a large, high-traffic intersection in Sofia, Republic of Bulgaria.

Table 1. Technical characteristics of the used UAVs

Sensor	Uncooled VOx Microbolometer
Focal Length	Approx. 9 mm (35 mm Format Equivalent: Approx. 38 mm)
Sensor Resolution	640 × 512 @ 30 Hz
Accuracy of Thermal Temperature	Measurement: ±2°C or ±2%, Whichever is Greater
Scene Range	-20°C to 150°C (High Gain) -20°C to 450°C (Low Gain)
Digital Zoom	16X
Pixel Pitch	12 µm
Spectral Band	8 – 14 µm
Photo Format	R-JPEG
Video Format	MP4
Metering Method	Spot Meter, Area Measurement
FFC (Flat Field Correction)	Auto / Manual

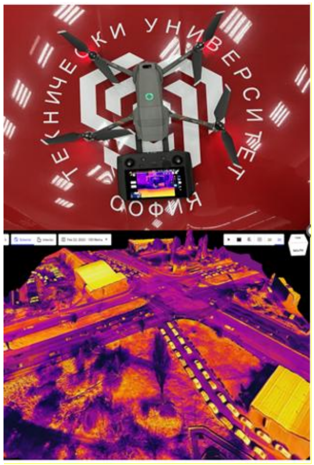

Although not included in the analysis, preliminary ground-based checks were conducted using a FLIR E40 handheld thermal camera to validate the general thermal behavior of the environment. While the FLIR E40 offers excellent point-specific thermal resolution for close-range inspections, the Mavic 2 Enterprise Advanced provides a significant advantage in spatial coverage and operational flexibility, making it ideal for capturing thermal dynamics across broader urban areas from above.

The object of the research is the intersection of GM Dimitrov Blvd. and Kliment Ohridski Blvd. in the city of Sofia, Republic of Bulgaria, with geographic coordinates 42°39'48.0"N 23°21'27.0"E according to Figure 1. The purpose of the research is by using the selected UAV to capture consecutive video images of the intersection, their subsequent processing with several digital photogrammetry and thermography software to determine the exact geometric and temperature characteristics of the infrastructure, the intersection itself and the captured vehicles. The choice of an intersection for conducting the study is complemented by the location of the intersection under consideration and its role in conducting traffic in the street network of the city of Sofia. It is a basic intersection in terms of its traffic load, which shows intensity values for each of the traffic flows that pass through it in the range between 500 and 800 vehicles per hour during peak periods of the day. The choice of the intersection is also complemented by the proven high density [68] of the traffic flows and measured values of the accelerations of the departing vehicles [69]. The intersection is light-regulated with the passage of traffic in four phases, where each branch is passed in a separate phase. These circumstances have their impact on the overall thermal impact, which confirms the choice of the studied intersection.

The effectiveness of thermal mapping heavily depends on the clarity, consistency, and lighting conditions during image acquisition. When utilizing UAVs for aerial thermographic surveys, optimal image quality is typically achieved around midday, when the sun is at or near its zenith. During this time, vertical solar illumination minimizes the presence of long shadows, which can obscure surface features and distort thermal readings.

In line with these considerations, the thermographic survey of the selected urban intersection is conducted between 12:10 and 12:30 local time on February 23, 2023. This time frame ensured consistent lighting and minimal shadow interference. Although the specific date was chosen at random, the flight represents part of a series of initial exploratory studies intended to inform a more comprehensive, long-term research effort focused on thermal monitoring of urban road infrastructure and vehicle activity using UAV-mounted sensors.

The environmental conditions during the flight were as follows: mostly cloudy skies, ambient temperature of 14°C (with a perceived temperature of 13°C), east-northeast wind at 6 km/h, relative humidity at 48%, atmospheric pressure of 1015 hPa, and visibility extending up to 30 km. These moderate weather conditions provided a stable environment for UAV operation and contributed to the reliability of the thermal data collected.

Figure 1. Image of the surveyed intersection and UAV flight plan

The perimeter of the studied area is determined by entering precise benchmarks (coordinates), alongside the desired flight height, shooting trajectory, shooting angle, and the required minimum number of photos for the area of interest. In terms of aerial photography in this study, the choice of flight altitudes is critical. The lower the drone flies, the more detailed the captured images are. Given that the work is conducted in an urban environment, the obstacles during the drone's flight path are a primary consideration for reducing the likelihood of accidents. The process for intersecting the study area begins at 20 meters above ground level, progressively increasing to 25 meters, then to 50 meters, followed by 75 meters, and ultimately reaching 100 meters. This specification is dictated by the thermal camera used, accounting for the obstructions in the study area. As a result, five drone flights are conducted over the area under investigation. At each flight altitude, as illustrated in the Figure 2, the flight plans encompass all altitudes, alongside the sequence and number of images, the required overlap between successive images, the total photographing area, and the resolution of the processed images, represented as the number of centimeters per pixel. The camera settings remain in automatic mode during capturing. Within this urban study area, the following features can be observed: an intersection regulated by traffic lights, pedestrian pathways, a subway stop, underpasses to the stop, sidewalk spaces, and green areas with several trees, as well as a gas station located on the east-west side of the intersection. Two identical images are captured during the imaging process— normal and thermal images. After the flights and capturing, photogrammetry software processes the images to create a 3D thermal map of the intersection as shown at Figure 2.

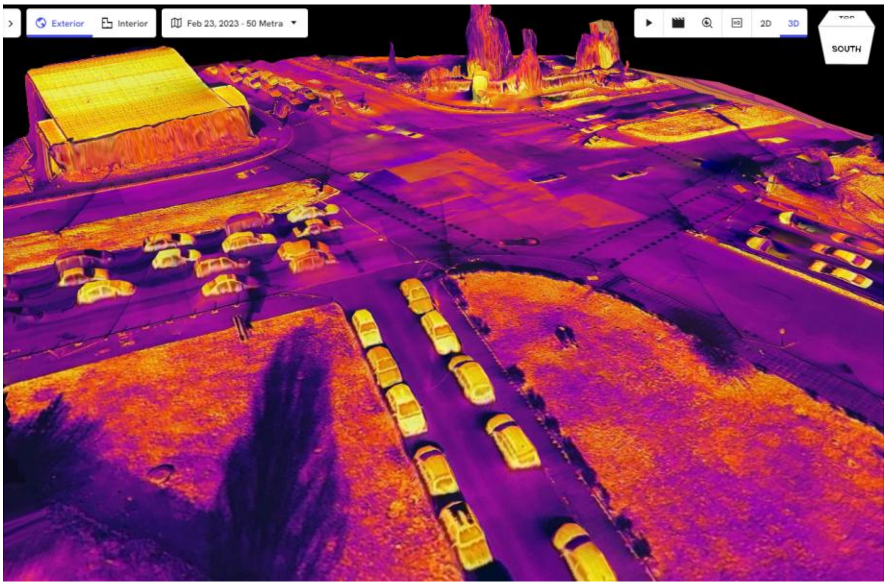

Figure 2. Thermal map of the intersection

The information needed to compose this thermo-photogrammetric map is detailed in Table 2.

Table 2. Details regarding the data utilized by the photogrammetric software

Photogrammetry Engine	***DroneDeploy* Proprietary**				
Date of Capture	Feb 23, 2023				
Date Processed	May 02, 2023				
Image Sensors	DJI – MAVIC 3 Enterprise – Advanced				
Average GPS Trust	10.00 m				
Flight Altitude	20	25	50	75	100
GSD Orthomosaic cm/px (GSD DEM cm/px)	1.32 (±5.8)	1.65 (±6.50)	3.10 (±3.22)	4.96 (±0.95)	6.34 (±3.25)
Area Bounds (m²)	135848.48 (47.9%)	152008.69 (52.3%)	109353.06 (75.4%)	177585.08 (82.0%)	250720.98 (84.0%)
Images Uploaded	197 (100%)	154 (100%)	193 (100%)	130 (100%)	26 (100%)
Camera Optimization	Principal Point Varied from reference value by 12.34%	Principal Point Varied from reference value by 10.15% Focal Length Varied from reference value by 9.03%	Principal Point Varied from reference value by 5.10% Focal Length Varied from reference value by 17.39%	Principal Point Varied from reference value by 5.91% Focal Length Varied from reference value by 5.89%	Focal Length Varied from reference value by 15.75%
Image Resolution	640 × 512 (~0.33 MP)				
Orthomosaic Coverage (% of area of interest)	47.71	52.38	75.40	82.04	84.09
Average Orthomosaic Image Density within Structured Area	5 images/pixel				
Aligned Cameras	197/197	154/154	49/49	30/30	26/26
RMSE of Camera GPS Location (m)	X: 0.19, Y: 0.24, Z: 0.27 RMSE 0.24	X: 0.16, Y: 0.17, Z: 0.23 RMSE 0.19	X: 0.53, Y: 0.43, Z: 0.33 RMSE 0.43	X: 0.52, Y: 0.50, Z: 0.22 RMSE 0.44	X: 0.43, Y: 0.42, Z: 0.34 RMSE 0.40
Nadir Images	100% Include oblique or horizontal images to improve reconstructions of man-made structures				
Oblique Images	0%	0%	0%	0%	0%
Horizontal Images	0%	0%	0%	0%	0%
Total Points (thousand)	757.7	689.3	464.8	317.3	282.1
Point Cloud Density (points/m²)	116.91	86.58	41.00	21.75	13.38
Mesh Triangles (thousand)	168.7	139.7	49.6	31.3	25.4
DEM GSD (cm/px)	5.28	6.50	13.22	19.85	25.36

Table 2 summarizes key parameters and outcomes from the photogrammetric processing of thermal imagery captured by the DJI Mavic 2 Enterprise Advanced UAV at five different flight altitudes (20 m, 25 m, 50 m, 75 m, and 100 m). These parameters are critical for understanding both the quality of the 3D reconstruction and the practical limitations of UAV-based thermal mapping in urban environments.

One of the most evident trends is the relationship between flight altitude and image coverage. As the altitude increases, the ground sampling distance (GSD) also rises—from 1.32 cm/pixel at 20 m to 6.34 cm/pixel at 100 m. This leads to lower spatial resolution at higher altitudes, but it enables the UAV to capture larger areas with fewer images. For instance, at 20 meters, 197 images were captured to cover approximately 13,584.98 m² (47% of the area of interest), whereas at 100 meters, only 26 images were needed to cover 25,072.90 m² (84% coverage). This trade-off between detail and coverage is essential in mission planning: lower altitudes are more suitable for high-resolution studies, such as defect detection in infrastructure, while higher altitudes are better for broader environmental mapping.

Despite variations in the altitude and the number of images, the alignment rate remained at 100% in all instances, demonstrating excellent flight stability, precise GPS tracking, and robust image quality—all crucial elements for successful photogrammetric reconstruction. The Root Mean Square Error (RMSE) of the camera GPS position stayed below 0.5 meters in all flights, with the lowest error recorded at 25 meters (RMSE = 0.19 m), indicating that this altitude may provide an optimal balance between image resolution and GPS reliability under the tested conditions.

The resolution and density of orthomosaic images vary significantly with the altitude. At lower altitudes, the image density is higher—for instance, the point cloud density reaches 116.91 points/m² at 20 meters, while it drops to only 13.38 points/m² at 100 meters. Similarly, mesh triangle counts decrease drastically, from 168.7 thousand triangles at 20 meters to just 25.4 thousand at 100 meters. This reduction in geometric detail could impact the accuracy of thermal mapping when identifying finer features (e.g., small cracks, pipe outlines, or narrow road markings).

The orthomosaic coverage, expressed as a percentage of the area of interest, increases with altitude due to the widening field of view. It ranges from 47.71% at 20 m to 84.09% at 100 m, confirming that higher altitudes are more efficient for broad coverage missions. However, the increase in GSD (up to 6.34 cm/pixel) at higher altitudes limits the granularity of thermal details, which could be critical depending on the application, such as traffic heat emissions versus micro-crack detection in pavements.

Camera calibration results—specifically, deviations in the principal point and focal length—also indicate slight variations at each altitude, which the software successfully compensated for. These differences are natural due to lens dynamics and UAV movement, and they do not seem to compromise image alignment or final output quality.

These findings are particularly relevant for smart city planning, traffic heat monitoring, and infrastructure diagnostics, where balancing resolution, area coverage, and processing resources is key to effective UAV-based thermal surveying.

The effective thermogrammetric analysis requires to take into account several factors, such as atmospheric conditions; the presence of smoke, dust, and air pollution; the emissivity coefficient; the transparency and reflectivity of captured elements; the time of day; the shooting angle; the type of paint, color, and surface finish of the objects in the photo; and the distance (in this case, shooting height) from the target. In addition to thermal energy and shape, roughness or smoothness will be considered extensively to provide an accurate picture of the thermal properties of an object or landscape. The radiation coefficient values of the materials mainly focused on in this study are shown in Table 3 [68, 67].

Table 3. Emissivity of various substances

Materials	Emissivity
Asphalt	0.97
Water	0.95
Iron	0.94
Polished aluminium	0.03
Cement	0.96
Basalt	0.72
Concrete	0.94
White paper	0.94
White paint	0.90
Black paint	0.98
Wood	0.85
Vegetation	0.94

In blackbody theory, the radiative properties of matter are assumed to be ideal regarding radiation. This radiation is described very well by Planck's law.

$$L_\lambda = \frac{2h\nu^3}{c^2}\frac{1}{e^{h\nu/kT}-1} \quad (1)$$

where L_λ is spectral radiance of a body; h is 6.62606876(52) ×10^{-34} J s (7.8 × 10^{-8}) (Planck constant); k is 1.3806503(24) × 10^{-23} J/K (1.7 × 10^{-6}) (Boltzmann constant); T is absolute temperature; ν is frequency; c is Speed of light in a vacuum.

In fact, all substances except idealized absolute black bodies above 0 K radiate differently. Therefore, the emissivity of a given substance is also an important property. Emissivity ε, defined as "the ratio of the emissivity of a body to the emissivity of an absolute black body", is a key concept:

$$\varepsilon(\lambda, \Theta, \varphi) = \frac{L_\lambda(\Theta,\varphi)}{L_{\lambda BB}} \quad (2)$$

This equation includes the directional component (Θ, φ).

The emissivity may be seen as a measure indicating a substance's ability to emit heat, with values ranging from 0 to 1. When it is neutral concerning wavelength and ε is less than 1, it is referred to as a gray body. Emissivity pertains to the characteristics of a specific sample, where ε (λ) is defined at a particular wavelength [70-72]. Lots of material properties may be 'flat' in one part of the spectrum but vary significantly at different wavelengths in another region. Since these properties are defined by functions, the values become insignificant in spectral regions where the function's value is negligible. For example, the transmittance of standard window glass is approximately 0.92 in the visible range but drops to zero in the infrared range, where the eye does not respond. Materials that have high reflectivity at short wavelengths do not absorb much radiation. If the reflectivity is low at longer wavelengths, the absorption rate will increase and consequently, thermal radiation will be greater [73, 74].

The processed thermal images are captured using software, and the capture conditions such as altitude, ambient temperature, and humidity are recorded for all processed images. The following data parameters are documented for the analysis: photo number, capture height, minimum temperature, maximum temperature, and weighted average temperature of the image field. During the processing of the images, very high positive and very low negative extreme values require extra check by an operator. After identifying the sources of these temperature anomalies (mainly reflections of the sun's rays) on the vehicle windows, road signs, brackets for traffic control cameras, and so on, these images are not used in the study.

At the output of the software processing, the maximum temperature, minimum temperature, and weighted average temperature values of the captured images are generated. Figure 3 and Table 2 present the image data, while Table 4 summarizes the data from the images. A total of 456 images are processed across all heights (20 meters - 197 images; 25 meters - 154 images; 50 meters - 49 images; 75 meters- 30 images; 100 meters - 26 images). The table provides average temperature values for the total number of images at different heights of the thermal images.

Table 4. Determined temperatures at the corresponding heights of the study

Distance (m)	Maximum Values (°C)			Minimum Values (°C)			Average Values (°C)		
	Max	Min	Average	Max	Min	Average	Max	Min	Average
20	88.0	20.0	45.04	32.5	-23.9	3.24	58.5	9.7	20.36
25	84.3	22.6	46.38	16.3	-23.9	2.21	49.7	12.4	20.96
50	60.4	34.9	47.91	9.9	-12.7	1.99	33.2	16.6	20.77
75	74.8	37.4	51.94	11.1	-12.7	0.13	29.1	14.4	20.28
100	76.0	45.9	53.37	6.0	-10.0	1.48	21.8	15.2	19.78

Figure 3 shows the minimum (orange line), maximum (blue line), and average (gray line) surface temperature values recorded during UAV-based thermographic measurements at flight altitudes from 20 m to 100 m.

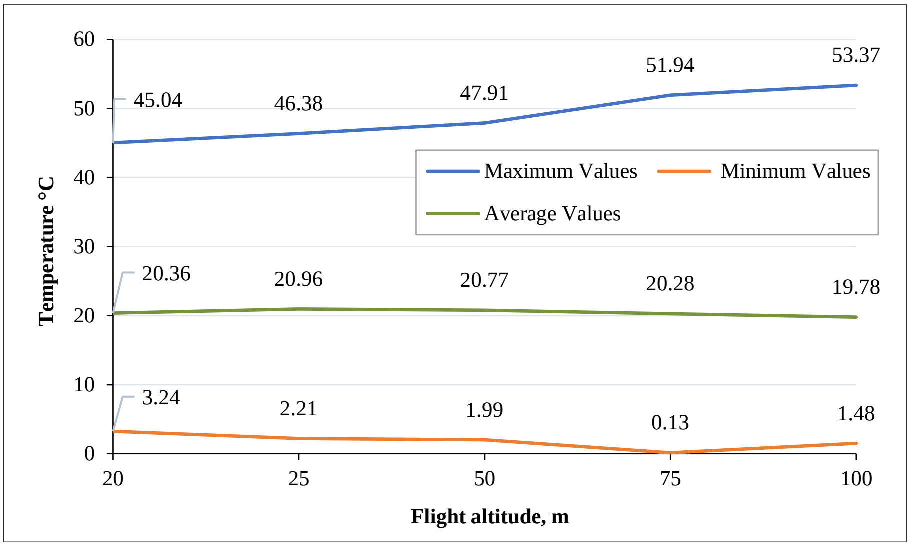

Figure 3. The minimum (orange line), maximum (blue line), and average (green line) temperature values for various heights in the study

- The maximum temperatures (blue line) exhibit a clear upward trend, rising from 45.04°C at 20 m to 53.37°C at 100 m. This indicates that higher altitudes enable the thermal camera to capture larger and potentially more exposed areas, including hotter surfaces or reflective elements (e.g., vehicle roofs or asphalt directly illuminated by the sun).
- The average temperatures (gray line) remain relatively stable, fluctuating slightly around 20°C. This indicates that, despite altitude changes, the general thermal background of the intersection remains consistent.
- The minimum temperatures (orange line) show a non-linear trend, initially decreasing from 3.24°C at 20 m to a minimum of 0.13°C at 75 m, before slightly increasing to 1.48°C at 100 m. This drop may be attributed to the increased prominence of shaded or cooler elements (e.g., tree canopies, metal surfaces in shadow) within the field of view at higher altitudes.

These data confirm that flight altitude affects thermal readings, particularly for maximum temperature values. The results support the idea that the UAV thermography benefits from multi-altitude scanning, providing a more nuanced thermal profile of urban intersections. This approach improves the accuracy of heat mapping and facilitates detailed analysis in smart city and traffic management contexts.

Figure 4 illustrates the average surface temperatures derived from thermographic images captured at five different UAV flight altitudes: 20 m, 25 m, 50 m, 75 m, and 100 m. The overall thermal profiles remain relatively consistent across all altitudes, demonstrating the stability and reliability of temperature measurements during the UAV flights.

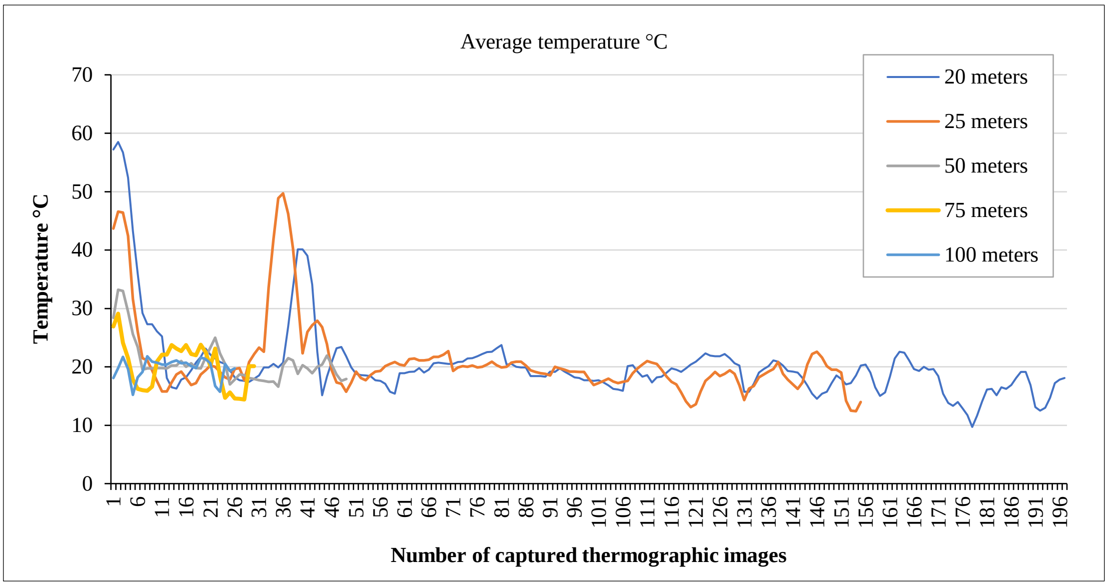

Figure 4. Trend in measured temperatures – 20. 25, 50, 75 and 100 meters

A distinct temperature peak is observed across all altitude profiles during the early part of the flight path. This anomaly corresponds to the large roof structure of the G.M. Dimitrov metro station, located within the monitored street intersection. The elevated thermal signature of the roof – likely a result of its material composition and prolonged sun exposure—stands out clearly against the surrounding urban surfaces. The thermal scanning sequence notably begins over this high-temperature zone, reflected in the prominent early spikes on the graph. As the UAV moves beyond this area, a gradual decrease in average surface temperatures is recorded, indicating a transition from the thermally dominant metro station to the cooler elements of the road and sidewalk.

This result underscores the sensitivity of UAV-based thermography in identifying localized heat sources within complex urban environments and reinforces the method's value in urban heat monitoring, infrastructure assessment, and smart city applications.

When examining individual components of the studied area road junction, temperatures shown by both the road infrastructure and the surrounding intersection (as illustrated at Figure 5) are evident. In the grassy areas and on most of the asphalt surface, the average temperatures are around 20°C, while lower temperatures are observed in certain sections of the street network.

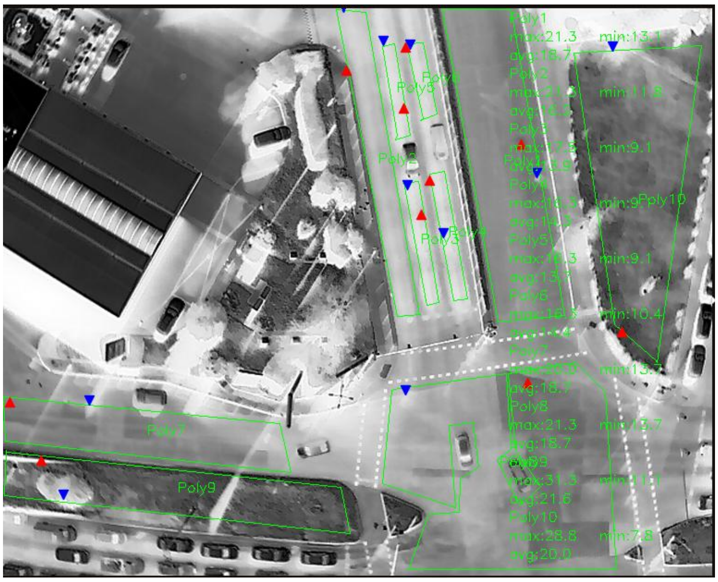

Figure 5. Determined temperatures of the road intersection.

A detailed study of the road layout and thermal imaging conditions reveals several factors. The average temperature in the vicinity of the junction is approximately 20°C, as the asphalt absorbs enough heat from the sunlight (the image is taken around midday) and, generally, this aligns with the direction of travel of the developed area being examined. The notable difference in the temperature of the asphalt results mainly from variations in its color shade and texture (Figure 6).

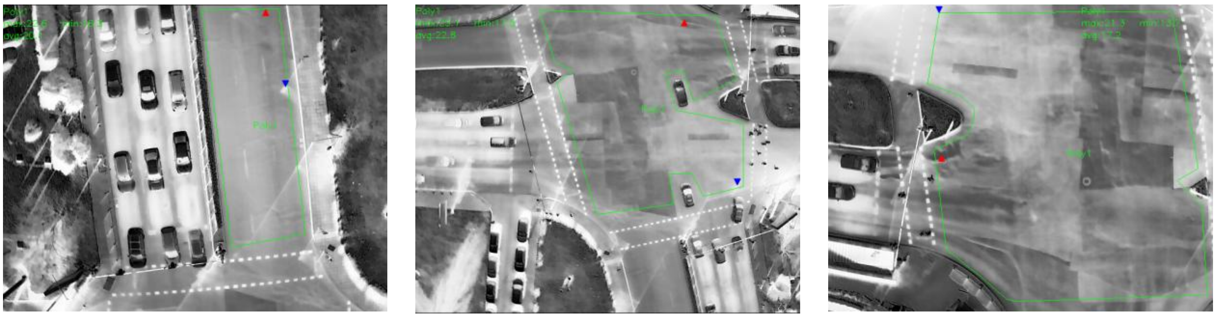

Figure 6. Average temperature of unoccupied areas of the road infrastructure

Note that in sections of the road structure where the asphalt is uniformly distributed without patches or clear irregularities, the temperature of the coating remains relatively constant across the entire studied area and in both the lengthwise and widthwise directions of the street lane, unaffected by the recording height (Figure 7).

Nearby the traffic lights, the temperatures may reach from 11°C to 14°C, which is significantly higher than the 10°C, which is observed at low temperatures for the remaining asphalt road not sheltered by the vehicles. The lower temperature readings are attributed to the cool night and daytime temperatures during the study, as the temperatures recorded in the areas where vehicles are parked are nearly identical to the daytime temperature at the time the images are captured as the asphalt is not heated by sunlight. The photographs taken from heights of 20, 25, and 50 meters clearly illustrate the temperature trace (shade) of vehicles on the road (Figure 8).

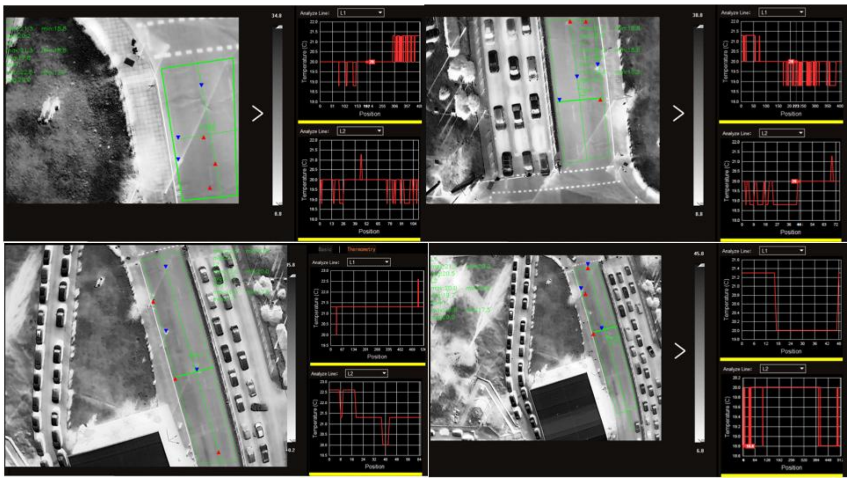

Figure 7. The temperature of areas of the road infrastructure

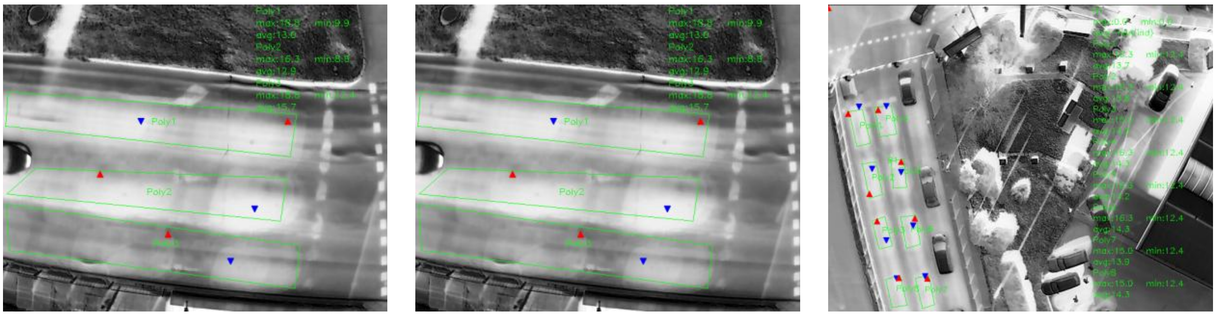

Figure 8. Temperature footprint (shadow) of waiting vehicles

Figure 8 also represents that the vehicle configurations have an influence to the temperature profile. The evaluation of vehicle images at this major road intersection indicates that general vehicle conditions cannot be determined through UAV and aerial IRT imaging. The outside temperature emitted from the surfaces of stationary vehicles depends on several factors, including the type and color of the paint coating, the varnish applied to the paint, and the method of paint application such as single-layer or multi-layer. Figure 9 displays two stationary vehicles with a painted section of their roofs, which clearly showing that their emissions differ based on the vehicle's basic color, regardless of the capture height. On a dark vehicle, there is virtually no noticeable difference in emissions, whereas on a silver vehicle, the difference in emissions is quite apparent.

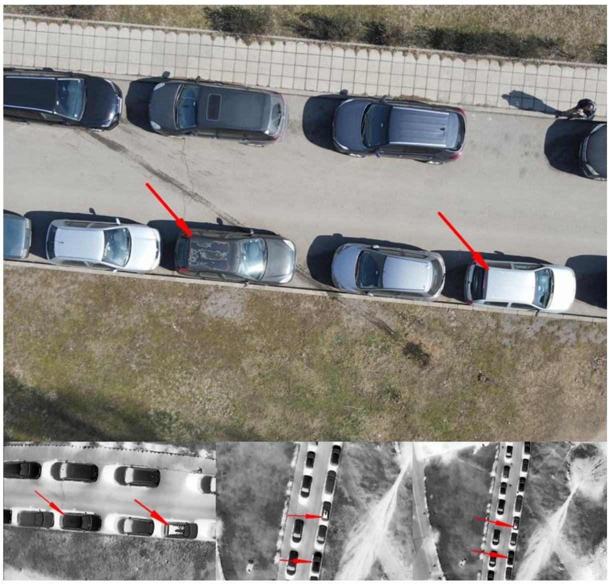

(a) (b) (c)

Figure 9. Photographed stationary vehicles from different distances: a) 25 meters; b) 50 meters; c) 75 meters

However, from the specified temperature, several conclusions may be drawn about emissions from individual vehicles, especially when the images are captured from a low angle, as they are very detailed. These images allow for the determination the both details - the general temperature distribution across the entire vehicle and the specific vehicle elements, which are visible in the image. Figure 10 displays images taken from a viewing height of 20 meters, which show that certain details of the vehicle bodies in the photographs have higher temperatures on the front cover. The engine is situated beneath that part of the vehicle. In this case, the greatest heat release originates precisely from the engine region.

Figure 10. Details of the higher temperature vehicles' bodies

For example, Figure 11 displays three vehicles with local heat sources. P1 and P2 points clearly indicate a raised windshield temperature of about 25°C, which is caused by the driver using the vehicle heater. Since the air stream is mostly directed toward the windshield, a small distinction within the blowing zones on the windshield is observed, likely due to the fact that the steam's air jet is optimally aimed at the driver and his line of sight. It also measures (P7 and P8 points) the vehicle headlight temperatures emitted by law for drivers to use their lights throughout the year in the Republic of Bulgaria, with the result being an approximate surface temperature of 35 °C in the headlights of all vehicles equipped with standard headlights rather than daytime running lights. The temperature of both headlights on each vehicle is consistent. Minor differences in the temperature distribution of the headlights among individual vehicles may be attributed to both the power and type of the light fixture, as well as the different materials used in the protective glass of the headlights themselves.

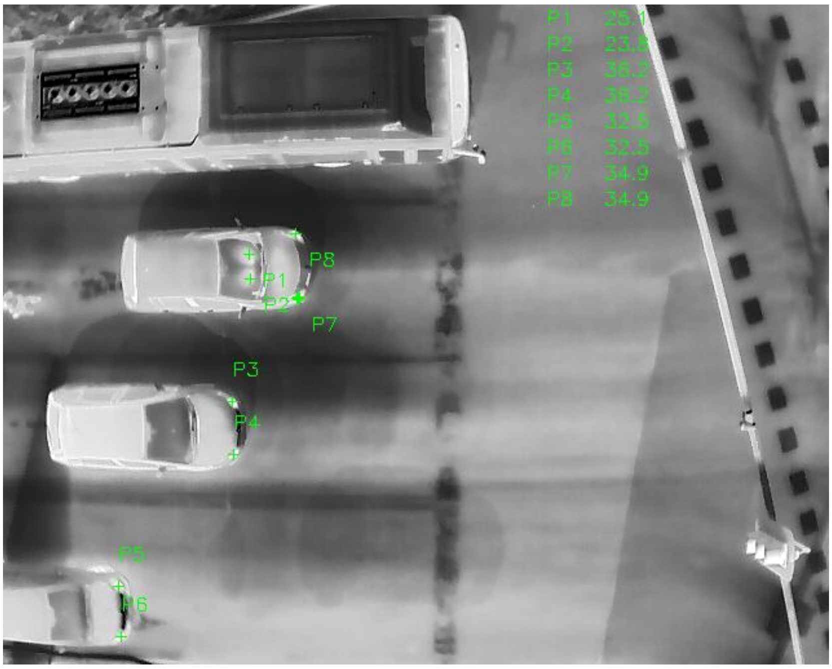

Figure 11. Vehicles with warmer windshields and headlights

4. Discussion

This study aims to determine the thermal load of a major urban street intersection within Sofia's city limits and to assess both the surface condition of the road infrastructure and the technical state of the vehicles crossing the intersection by utilizing airborne thermal images captured with the help of an unmanned aerial vehicle and thermo-photogrammetry analysis. It specifically addresses the basic steps taken to evaluate the thermal loading and surface coverage of both the vehicles and the infrastructure, quantifying their impact on the environment, atmosphere, and surface emissivity of the studied sites.

Most road surface and infrastructure conditions are usually assessed through visual examinations by road inspectors. This approach is limited due to the lack of comprehensive research and development, which can be costly and labor-intensive. Given the age and quality of road surfaces in the capital city and the country as a whole, it is increasingly necessary to develop cost-effective, non-destructive methods for innovative testing. Such methods would help determine the state of road infrastructure at specific intervals without interrupting traffic flow. The technologies that enable remote monitoring and diagnostics of transport infrastructure quality and condition are crucial, as they facilitate timely prevention measures. Asphalt is the most common type of road surface, and its service life correlates with the overall quality and condition of the infrastructure due to its affordability, alongside the ease of repair and maintenance. However, road infrastructure and asphalt surfaces are vulnerable to various factors that can lead to their deterioration, loss of strength, and damage. This directly impacts traffic safety, results in increased repair and operational costs, and causes significant inconveniences for drivers and passengers. Moreover, it affects the technical condition of vehicles, necessitating repairs that can further disrupt and degrade the urban environment.

From the research and analysis, it cannot be definitively stated that the road traffic contributes to the thermal load of the urban area. This is likely due to the decision to conduct the study during a cold month. However, as mentioned at the outset of this publication, this will serve as an excellent stepping stone for future progress in this area. The warming of the street and neighborhood infrastructure can only be facilitated by sunlight. Many more studies in a similar vein, conducted at different times of the year and under varying climatic conditions, are necessary. These studies will help build models that further support techniques for accurately defining the impact of road traffic on urban street environment conditions, precisely identifying sources of temperature rise, and implementing specific measures to reduce thermal loading. Further collaborative efforts must be undertaken to assess the environmental impact and air pollution at the busiest street intersections in individual cities and their infrastructures. Gathering extensive databases is essential for determining the actual state of the urban environment, road transport, and infrastructure, as well as for identifying exact sources of pollution to take targeted actions to neutralize these sources.

Artificial intelligence systems may also participate in processing thermal images, which helps circumvent most data processing problems. In this context, systems using deep learning and convolutional neural networks are recommended. Deep learning refers to the type of artificial intelligence that enables a person to automatically understand their environment by extracting information and learning facts using structures similar to convolutional neural networks (CNNs). Acquiring and analyzing data on a large scale generates insights into different class types, making them more distinguishable. With its own discovered patterns, the deep network may classify newly added image data into appropriate classes, allowing for the automated identification of objects. This process eliminates the need to provide an image matrix for every object, enabling conclusions to be drawn about a class based on all available image information, thereby improving identification efficiency. In recent years, large datasets and powerful computers have advanced deep convolutional neural networks (CNNs) [75-78], allowing them to outperform various traditional computer vision algorithms.

This approach effectively partitions regions of unknown object types based on different class training and testing. However, it can also suffer from overtraining in cases with common characteristics in the dataset, which may be less of an issue in factories handling a diverse sample of items across various categories. The learning capabilities exhibited by network structures that integrate AI and machine vision techniques not only inspire researchers but also support them in creating more intelligent automated systems in manufacturing.

5. Conclusion

The use of similar large-scale studies and research, employing thermal video recording from unmanned aerial vehicles and thermal cameras, can enhance the reliability and efficiency of studying and controlling road infrastructure in cities, the temperature load of the urban environment, and the technical condition of road vehicles in non-urban areas. Implementing these innovative research and monitoring methods for the road transport infrastructure in large cities and the urban environment will significantly improve quality of life and increase well-being for all citizens.

No conclusions or assumptions can be drawn about the general technical condition of the vehicles that passed through the studied intersection based on the research conducted and the goal established. This limitation arises from the aerial imagery used; adequate details regarding the vehicles' technical condition cannot be obtained from thermal images alone, only general assumptions can be made. Extensive photographic work must be performed on the vehicles from both aerial and ground levels to gather sufficient statistical facts for creating models that determine temperature deviations in relation to the vehicles' technical condition. To accurately examine the technical condition of individual vehicles, such research should ideally involve ground thermal imaging using multiple cameras installed on each vehicle. Combining both ground and aerial studies would be preferable for this type of research.

6. Declarations

6.1. Author Contributions

Conceptualization, I.D., G.M., and D.S.; methodology, I.D., D.S., and G.M.; software, I.D., K.D., R.M., and V.H.; validation, I.D., R.M., D.S., G.M., K.D., and V.H.; formal analysis, V.D., R.M., and K.D.; investigation, I.D., G.M., and D.S.; data curation, I.D., D.S., R.M., G.M., V.H., and G.M.; writing—original draft preparation, I.D.; writing—review and editing, I.D. and K.D.; funding acquisition, I.D. and K.D. All authors have read and agreed to the published version of the manuscript.

6.2. Data Availability Statement

The data presented in this study are available in the article.

6.3. Funding and Acknowledgements

The authors would like to thank the Research and Development Sector at the Technical University of Sofia for the financial support. The authors' collective would like to express our sincere gratitude to the Faculty of Transport and the Faculty of Telecommunications at the Technical University of Sofia for providing the laboratory base.

6.4. Conflicts of Interest

The authors declare no conflict of interest.

7. References

[1] Lancet Countdown. (2023). Heat-related Mortality. Lancet Countdown, London, United Kingdom. Available online: https://lancetcountdown.org/explore-our-data/ (accessed on April 2025).

[2] Zhao, Q., Guo, Y., Ye, T., Gasparrini, A., Tong, S., Overcenco, A., Urban, A., Schneider, A., Entezari, A., Vicedo-Cabrera, A. M., Zanobetti, A., Analitis, A., Zeka, A., Tobias, A., Nunes, B., Alahmad, B., Armstrong, B., Forsberg, B., Pan, S.-C., … Li, S. (2021). Global, regional, and national burden of mortality associated with non-optimal ambient temperatures from 2000 to 2019: a three-stage modelling study. The Lancet Planetary Health, 5(7), e415–e425. doi:10.1016/s2542-5196(21)00081-4.

[3] Ballester, J., Quijal-Zamorano, M., Méndez Turrubiates, R. F., Pegenaute, F., Herrmann, F. R., Robine, J. M., Basagaña, X., Tonne, C., Antó, J. M., & Achebak, H. (2023). Heat-related mortality in Europe during the summer of 2022. Nature Medicine, 29(7), 1857–1866. doi:10.1038/s41591-023-02419-z.

[4] Ebi, K. L., Capon, A., Berry, P., Broderick, C., de Dear, R., Havenith, G., Honda, Y., Kovats, R. S., Ma, W., Malik, A., Morris, N. B., Nybo, L., Seneviratne, S. I., Vanos, J., & Jay, O. (2021). Hot weather and heat extremes: health risks. The Lancet, 398(10301), 698–708. doi:10.1016/s0140-6736(21)01208-3.

[5] Batson, A. (2019). Road pavement acceptance during construction, Guide note. Department of Infrastructure Planning and Logistics, Northern Territory Government, Darwin, Australia.

[6] Freeman, R. B., & Grogan, W. P. (1998). Statistical Acceptance Plan for Asphalt Pavement Construction. Defense Technical Information Center, Fort Belvoir, Virginia, United States. doi:10.21236/ada347907.

[7] Department for Transport. (2021). Road Condition Data and Technology Review: Position Paper, Research and analysis. Department for Transport, London, United Kingdom.

[8] Leigh, A., & Neill, C. (2011). Can national infrastructure spending reduce local unemployment? Evidence from an Australian roads program. Economics Letters, 113(2), 150–153. doi:10.1016/j.econlet.2011.05.037.

[9] Jenelius, E., & Mattsson, L. G. (2015). Road network vulnerability analysis: Conceptualization, implementation and application. Computers, Environment and Urban Systems, 49, 136–147. doi:10.1016/j.compenvurbsys.2014.02.003.

[10] Qiang, Q., & Nagurney, A. (2008). A unified network performance measure with importance identification and the ranking of network components. Optimization Letters, 2(1), 127–142. doi:10.1007/s11590-007-0049-2.

[11] Sullivan, J. L., Novak, D. C., Aultman-Hall, L., & Scott, D. M. (2010). Identifying critical road segments and measuring system-wide robustness in transportation networks with isolating links: A link-based capacity-reduction approach. Transportation Research Part A: Policy and Practice, 44(5), 323–336. doi:10.1016/j.tra.2010.02.003.

[12] Taylor, M. A. P., & Susilawati. (2012). Remoteness and accessibility in the vulnerability analysis of regional road networks. Transportation Research Part A: Policy and Practice, 46(5), 761–771. doi:10.1016/j.tra.2012.02.008.

[13] Blom, C. M., & Guthrie, P. M. (2015). Surveying customer perceptions of road infrastructure comfort. Infrastructure Asset Management, 2(4), 173–185. doi:10.1680/jinam.15.00007.

[14] Tarigan, H., Matondang, A. R., Lubis, S., & Sirojuzilam, S. (2021). The Effect of Road Transportation Infrastructure on Freight Transport Mobility and Regional Economy in Indonesia. Journal of Asian Finance, Economics and Business, 8(3), 645–654. doi:10.13106/jafeb.2021.vol8.no3.0645.

[15] Desmet, K., & Henderson, J. V. (2015). The Geography of Development within Countries. Handbook of Regional and Urban Economics, 1457–1517, Elsevier, Amsterdam, Netherland. doi:10.1016/b978-0-444-59531-7.00022-3.

[16] VTPI. (2020). Online TDM Encyclopedia. Victoria Transport Policy Institute, Victoria, Canada. Available online: https://www.vtpi.org/tdm/ (accessed on April 2025).

[17] Mindell, J. S., & Birley, M. (2020). Qualitative health impact assessment. Traffic-Related Air Pollution, 311–337, Elsevier, Amsterdam, Netherland. doi:10.1016/b978-0-12-818122-5.00012-0.

[18] Negev, M., Levine, H., Davidovitch, N., Bhatia, R., & Mindell, J. (2012). Integration of health and environment through health impact assessment: Cases from three continents. Environmental Research, 114, 60–67. doi:10.1016/j.envres.2012.02.003.

[19] Papp, C. R., & Berchi, G. M. (2019). State of the art report and gap analysis in the field of environmentally-friendly transport infrastructure development. Danube Transnational Programme TRANSGREEN Project-WWF Romania, Budapest, Hungary.

[20] Decae, R., Goldenbeld, C., & Hermens, f. (2021). Road safety targets Monitoring report, Version 1.1, May 2021, Reporting period 2000-2020. European Road Safety Observatory, Brussels, Belgium.

[21] World Health Organization (WHO). (2016). Post-crash response Supporting those affected by road traffic crashes. World Health Organization (WHO), Geneva, Switzerland.

[22] European Commission. (2018). Post-impact Care. Directorate General for Transport, European Commission, Brussels, Belgium.

[23] A/RES/74/299. (2020). Resolution adopted by the General Assembly on 31 August 2020. Seventy-fourth Session, Improving Global Road Safety, United Nations, New York, United States.

[24] W.H.O. (2021). Decade of Action for Road Safety 2021-2030. World Health Organization (WHO), Geneva, Switzerland.

[25] Speight, J. G. (2016). Asphalt Chemistry. Asphalt Materials Science and Technology, 253–301, Butterworth-Heinemann, Oxford, United Kingdom. doi:10.1016/b978-0-12-800273-5.00006-4.

[26] Sulyman, M., Sienkiewicz, M., & Haponiuk, J. (2014). Asphalt Pavement Material Improvement: A Review. International Journal of Environmental Science and Development, 5(5), 444–454. doi:10.7763/ijesd.2014.v5.525.

[27] Almeida, A., & Picado-Santos, L. (2022). Asphalt Road Pavements to Address Climate Change Challenges—An Overview. Applied Sciences (Switzerland), 12(24), 12515. doi:10.3390/app122412515.

[28] Krishnan, J. M., & Rajagopal, K. R. (2005). On the mechanical behavior of asphalt. Mechanics of Materials, 37(11), 1085–1100. doi:10.1016/j.mechmat.2004.09.005.

[29] Zhang, C., Tan, Y., Gao, Y., Fu, Y., Li, J., Li, S., & Zhou, X. (2022). Resilience assessment of asphalt pavement rutting under climate change. Transportation Research Part D: Transport and Environment, 109, 103395. doi:10.1016/j.trd.2022.103395.

[30] Gudipudi, P. P., Underwood, B. S., & Zalghout, A. (2017). Impact of climate change on pavement structural performance in the United States. Transportation Research Part D: Transport and Environment, 57, 172–184. doi:10.1016/j.trd.2017.09.022.

[31] Guo, R., Nian, T., & zhou, F. (2020). Analysis of factors that influence anti-rutting performance of asphalt pavement. Construction and Building Materials, 254. doi:10.1016/j.conbuildmat.2020.119237.

[32] Vyas, V., Patil, V. J., Singh, A. P., & Srivastava, A. (2019). Application of infrared thermography for debonding detection in asphalt pavements. Journal of Civil Structural Health Monitoring, 9(3), 325–337. doi:10.1007/s13349-019-00337-8.

[33] Vyas, V., Patil, V. J., Singh, A. P., & Anshuman, A. (2020). Debonding detection in asphalt pavements using infrared thermography. Transportation Research Procedia, 48(2), 3850–3859. doi:10.1016/j.trpro.2020.08.035.

[34] Garg, S., & Misra, S. (2021). Efficiency of NDT techniques to detect voids in grouted post-tensioned concrete ducts. Nondestructive Testing and Evaluation, 36(4), 366-387. doi:10.1080/10589759.2020.1758100.

[35] Vyas, V., & Singh, A. P. (2022). Modeling asphalt pavement condition using artificial neural networks. Materials Today: Proceedings, 62, 1671-1676. doi:10.1016/j.matpr.2022.05.050.

[36] Li, P., Wang, Z., Men, B., Ma, X., Tang, G., & Wang, R. (2023). Use of Multi-Scale Investigation to Evaluate Adhesion Performance of Warm-Mix Polymer-Modified Asphalt. Materials, 16(1), 287. doi:10.3390/ma16010287.

[37] Yun, J., Vigneswaran, S., Lee, M. S., Choi, P., & Lee, S. J. (2023). Effect of Blending and Curing Conditions on the Storage Stability of Rubberized Asphalt Binders. Materials, 16(3), 978. doi:10.3390/ma16030978.

[38] Radziszewski, P., Liphardt, A., Sarnowski, M., Kowalski, K. J., Pokorski, P., Konieczna, K., Król, J. B., Iwański, M., Chomicz-Kowalska, A., Maciejewski, K., Iwański, M. M., & Michalec, M. (2023). Ageing Evaluation of Foamed Polymer Modified Bitumen with Bio-Flux Additive. Materials, 16(6), 2197. doi:10.3390/ma16062167.

[39] Bocci, E., Prosperi, E., Mair, V., & Bocci, M. (2020). Ageing and cooling of hot-mix-asphalt during hauling and paving—a laboratory and site study. Sustainability (Switzerland), 12(20), 1–16. doi:10.3390/su12208612.

[40] Phaltane, P. P. (2016). Effects of Temperature Segregation on the Denisity and Mechanical Properties of Asphalt Mixtures. Master Thesis, Louisiana State University and Agricultural & Mechanical College, Baton Rouge, United States. doi:10.31390/gradschool_theses.4477.

[41] Lavin, P. (2003). Asphalt pavements: a practical guide to design, production and maintenance for engineers and architects. CRC Press, London, United Kingdom. doi:10.1201/9781482267716.

[42] Milad, A. A., Adwan, I., Majeed, S. A., Memon, Z. A., Bilema, M., Omar, H. A., Abdolrasol, M. G. M., Usman, A., & Yusoff, N. I. M. (2021). Development of a Hybrid Machine Learning Model for Asphalt Pavement Temperature Prediction. IEEE Access, 9, 158041–158056. doi:10.1109/access.2021.3129979.

[43] Wang, X., Pan, P., & Li, J. (2023). Real-time measurement on dynamic temperature variation of asphalt pavement using machine learning. Measurement: Journal of the International Measurement Confederation, 207. doi:10.1016/j.measurement.2022.112413.

[44] Aljagoub, D., Na, R., Cheng, C., & Shen, Z. (2022). Performance Evaluation of Uncooled UAV Infrared Camera in Detecting Concrete Delamination. Infrastructures, 7(12), 163. doi:10.3390/infrastructures7120163.

[45] Japan International Cooperation Agency. (2013). Information Collection and Confirmation Survey on Road and Bridge Maintenance Management. Japan International Cooperation Agency, Tokyo, Japan.

[46] Mac, V. H., Huh, J., Doan, N. S., Shin, G., & Lee, B. Y. (2020). Thermography-based deterioration detection in concrete bridge girders strengthened with carbon fiber-reinforced polymer. Sensors (Switzerland), 20(11), 1–19. doi:10.3390/s20113263.

[47] Janků, M., & Stryk, J. (2017). Application of infrared camera to bituminous concrete pavements: Measuring vehicle. IOP Conference Series: Materials Science and Engineering, 236(1), 12104. doi:10.1088/1757-899X/236/1/012104.

[48] Omar, T., & Nehdi, M. L. (2017). Thermal detection of subsurface delaminations in reinforced concrete bridge decks using unmanned aerial vehicle. SP-331: Durability of Concrete Structures Incorporating Conventional and Advanced Materials, 1-14. doi:10.14359/51715590.

[49] Ojeda, J. M. P., Huatangari, L. Q., Calderon, B. A. C., Tineo, J. L. P., Panca, C. Z. A., & Pino, M. E. M. (2024). Estimation of the Physical Progress of Work Using UAV and BIM in Construction Projects. Civil Engineering Journal, 10(2), 362-383. doi:10.28991/CEJ-2024-010-02-02.

[50] Worachairungreung, M., Kulpanich, N., Sae-ngow, P., Thanakunwutthirot, K., Anurak, K., & Hemwan, P. (2024). Classification of Coconut Trees Within Plantations from UAV Images Using Deep Learning with Faster R-CNN and Mask R-CNN. Journal of Human, Earth, and Future, 5(4), 560-573. doi:10.28991/HEF-2024-05-04-02.

[51] Lee, S., Moon, H., Choi, Y., & Yoon, D. K. (2018). Analyzing thermal characteristics of urban streets using a thermal imaging camera: A case study on commercial streets in Seoul, Korea. Sustainability (Switzerland), 10(2), 519. doi:10.3390/su10020519.

[52] Yamazaki, F., Murakoshi, A., & Sekiya, N. (2009). Observation of urban heat island using airborne thermal sensors. 2009 Joint Urban Remote Sensing Event, 1-5. doi:10.1109/URS.2009.5137723.

[53] Dekić, J. P., Mitković, P. B., Dinic Branković, M. M., Igić, M. Z., Dekić, P. S., & Mitković, M. P. (2018). The study of effects of greenery on temperature reduction in urban areas. Thermal Science, 988-1000. doi:10.2298/TSCI170530122D.

[54] Kong, F., Yin, H., James, P., Hutyra, L. R., & He, H. S. (2014). Effects of spatial pattern of greenspace on urban cooling in a large metropolitan area of eastern China. Landscape and Urban Planning, 128, 35–47. doi:10.1016/j.landurbplan.2014.04.018.

[55] Zhang, Q., Zhou, D., Xu, D., Cheng, J., & Rogora, A. (2022). Influencing factors of the thermal environment of urban green space. Heliyon, 8(11), e11559. doi:10.1016/j.heliyon.2022.e11559.

[56] Weber, N., Haase, D., & Franck, U. (2014). Zooming into temperature conditions in the city of Leipzig: How do urban built and green structures influence earth surface temperatures in the city? Science of the Total Environment, 496, 289–298. doi:10.1016/j.scitotenv.2014.06.144.

[57] Roxon, J., Ulm, F. J., & Pellenq, R. J. M. (2020). Urban heat island impact on state residential energy cost and CO_2 emissions in the United States. Urban Climate, 31. doi:10.1016/j.uclim.2019.100546.

[58] Pham Xuan, R., Xiong, Y., Brietzke, A., & Marker, S. (2021). Thermal infrared imaging based facial temperature in comparison to ear temperature during a real-driving scenario. Journal of Thermal Biology, 96. doi:10.1016/j.jtherbio.2020.102806.

[59] Mirones Gómez, B. J. (2021). Thermal comfort in conventional vehicles (ICE) and electric (EV)-Evaluation Methods. Transportation Research Procedia, 58, 662–669. doi:10.1016/j.trpro.2021.11.087.

[60] Afrin, T., Yodo, N., Dey, A., & Aragon, L. G. (2024). Advancements in UAV-Enabled Intelligent Transportation Systems: A Three-Layered Framework and Future Directions. Applied Sciences (Switzerland), 14(20), 9455. doi:10.3390/app14209455.

[61] Bhadoriya, A. S., Vegamoor, V., & Rathinam, S. (2022). Vehicle Detection and Tracking Using Thermal Cameras in Adverse Visibility Conditions. Sensors, 22(12), 4567. doi:10.3390/s22124567.

[62] Tichý, T., Švorc, D., Růžička, M., & Bělinová, Z. (2021). Thermal feature detection of vehicle categories in the urban area. Sustainability (Switzerland), 13(12), 6873. doi:10.3390/su13126873.

[63] Askarzadeh, T., Bridgelall, R., & Tolliver, D. D. (2025). Drones for Road Condition Monitoring: Applications and Benefits. Journal of Transportation Engineering, Part B: Pavements, 151(1), 04024055. doi:10.1061/jpeodx.pveng-1559.

[64] Choi, J. D., & Kim, M. Y. (2023). A sensor fusion system with thermal infrared camera and LiDAR for autonomous vehicles and deep learning based object detection. ICT Express, 9(2), 222–227. doi:10.1016/j.icte.2021.12.016.

[65] Yoon, S., & Cho, J. (2022). Deep Multimodal Detection in Reduced Visibility Using Thermal Depth Estimation for Autonomous Driving. Sensors, 22(14), 5084. doi:10.3390/s22145084.

[66] Zhang, Y., Carballo, A., Yang, H., & Takeda, K. (2023). Perception and sensing for autonomous vehicles under adverse weather conditions: A survey. ISPRS Journal of Photogrammetry and Remote Sensing, 196, 146–177. doi:10.1016/j.isprsjprs.2022.12.021.

[67] DJI (2025). Support for Mavic 2 Enterprise Advanced. DJI, Shenzhen, China. Available online: https://enterprise.dji.com/mavic-2-enterprise-advanced (accessed on April 2025).

[68] Saliev, D. N., & Damyanov, I. S. (2024). Traffic flow density study at traffic light junction. AIP Conference Proceedings, 3078(1), 50004. doi:10.1063/5.0208304.

[69] Saliev, D. N., & Damyanov, I. S. (2022). Vehicles acceleration rate study for intergreen time of a signal cycle compute. AIP Conference Proceedings, 2449(1), 50007. doi:10.1063/5.0091882.

[70] Chen, W., Wei, K., Wei, J., Han, W., Zhang, X., Hu, G., Wei, S., Niu, L., Chen, K., Fu, Z., Xu, X., Xu, B., & Cui, T. (2022). Research on the Road Performance of Asphalt Mixtures Based on Infrared Thermography. Materials, 15(12), 4309. doi:10.3390/ma15124309.

[71] The Engineering ToolBox. (2003). Emissivity Coefficients of Common Materials: Data & Reference Guide. The Engineering ToolBox. Available online: https://www.engineeringtoolbox.com/emissivity-coefficients-d_447.html (accessed on April 2025).

[72] Palmer, J. M., & Grant, B. G. (2009). The art of radiometry. The international society for optics and photonics SPIE, Bellingham, United States. doi:10.1117/3.798237.

[73] Sapritsky, V., & Prokhorov, A. (2020). Blackbody Radiometry: Volume 1: Fundamentals. Springer Nature, Cham, Switzerland. doi:10.1007/978-3-030-57789-6.

[74] Wolfe, W. L. (1998). Introduction to radiometry (Vol. 29). SPIE Press, Bellingham, United States. doi:10.1117/3.287476.

[75] Parr, A. C., Datla, R., & Gardner, J. (2005). Optical Radiometry (Volume 41). Elsevier, Amsterdam, Netherlands.

[76] Howell, J. R., Mengüç, M. P., Daun, K., & Siegel, R. (2020). Thermal radiation heat transfer. CRC press, Boca Raton, United States. doi:10.1201/9780429327308.

[77] Liu, F., Liu, J., & Wang, L. (2022). Deep learning and infrared thermography for asphalt pavement crack severity classification. Automation in Construction, 140, 0926–5805. doi:10.1016/j.autcon.2022.104383.

[78] Kulkarni, N. N., Raisi, K., Valente, N. A., Benoit, J., Yu, T., & Sabato, A. (2023). Deep learning augmented infrared thermography for unmanned aerial vehicles structural health monitoring of roadways. Automation in Construction, 148. doi:10.1016/j.autcon.2023.104784.